Astron. Astrophys. 322, 296–301 (1997)

ASTRONOMY
AND
ASTROPHYSICS

Grain-grain collisions and sputtering in oblique C-type shocks

P. Caselli[1,2], **T.W. Hartquist**[2], **and O. Havnes**[3]

[1] Osservatorio Astrofisico di Arcetri, Largo E. Fermi 5, I-50125 Firenze, Italy
[2] Max-Planck-Institut für extraterrestrische Physik, D-85740 Garching, Germany
[3] Auroral Observatory, University of Tromsø, N-9037 Tromsø, Norway

Received 29 August 1996 / Accepted 13 November 1996

Abstract. We use a model of the dissipation regions in C-type shocks in which two grain fluids are included to evaluate the rates at which grain-grain collisions and sputtering inject elemental silicon and water into the gas phase. For physical parameters typical of star forming regions, and on the assumption that a substantial fraction of the evaporated silicon is efficiently converted in SiO, the two grain destruction mechanisms lead to gas phase SiO abundances larger than those in the quiescent gas by more than three orders of magnitude. This result is in good agreement with recent observations of SiO near stellar jets. Grain-grain collisions will dominate the return of elemental silicon to the gas phase when the hydrogen nuclei number density of the region into which the shock is propagating is $n_{\rm Ho} \gtrsim 5 \times 10^5\,{\rm cm}^{-3}$ and the shock speed is between about 25 km s^{-1} and 35 km s^{-1}. Grain-grain collisions dominate over sputtering in the return of water to the gas phase when $n_{\rm Ho} \gtrsim 10^6\,{\rm cm}^{-3}$ and at some shock speeds below about 15 km s^{-1}.

Key words: interstellar medium: clouds – interstellar medium: dust, extinction – physical processes: shock waves – interstellar medium: jets and outflows

1. Introduction

Gas phase SiO emission has been observed in clumpy structures along jets from young stellar objects embedded in low mass cloud cores (Mikami et al. 1992; Bally et al. 1993; Martín-Pintado et al. 1992; McMullin et al. 1994; Blake et al. 1995; Zhang et al. 1995; Avery & Chiao 1996) and in massive star forming regions (Downes et al. 1982; Wright et al. 1983; Martín-Pintado et al. 1992; Acord et al. 1996). On the other hand, only low upper limits of the SiO fractional abudance ($X_{\rm SiO} < 3 \times 10^{-12}$) have been inferred towards cold and quiescent clouds, such as TMC-1 (Ziurys et al. 1989). This suggests that silicon is heavily depleted in dense, quiescent clouds and that shock processing of dust grains releasing silicon-bearing species into the gas phase may be responsible for the SiO emission observed in star forming regions (e.g. Martín-Pintado et al. 1992).

If the SiO emission is associated with shocks, the velocity widths of the features are in harmony with those shocks being of C-type (Draine 1980). We may reasonably assume that each shock is propagating through an upstream molecular medium. Draine (1995), Flower & Pineau des Forêts (1995), and Schilke et al. (1996) have previously considered the release into the gas phase of silicon-bearing species as a consequence of sputtering induced by systemic grain-neutral streaming in such shocks. Draine et al. (1983) performed a similar analysis for water. A simplified treatment of grain-grain collisions in J-type shocks was first considered by Seab & Shull (1983). Recently, more detailed studies of grain destruction including grain-grain collisions and grain shattering in J-type shocks have been performed by Jones et al. (1994; 1996). These studies are restricted to steady state shocks in the warm intercloud component of the interstellar medium (number density $\simeq 0.25\,{\rm cm}^{-3}$; temperature $\simeq 10^4$ K). In this paper we present the first results for the release of silicon-bearing species and of water into the gas phase due to grain-grain collisions in C-type shocks in dark clouds and star forming regions, and first comparisons with sputtering rates.

To obtain these results we have considered for the first time models of the structures of shocks in dark molecular regions in which grains of more than one size are included. In order to investigate sputtering and grain-grain collisions for a wide range of parameter space, we have assumed that spatial variations within the long dissipation region of a C-type shock can be neglected and that the conditions throughout a large fraction of a dissipation region can be well approximated from the solution of a set of simultaneous algebraic equations. A comparable exploration of parameter space based on solutions of the ordinary differential equations governing shock structures in plane parallel models of steady oblique flows is currently computationally unfeasible.

In Sect. 2 we describe our calculations of the shock properties; our particular aim was the derivation of the typical grain-neutral and grain-grain relative speeds in the dissipation regions. In Sect. 3 we summarize briefly the results adopted from Tie-

Send offprint requests to: P. Caselli

lens et al. (1994) and from Draine & Salpeter (1979) to evaluate the yields of silicon-bearing species and of water from grain-grain collisions and sputtering. In Sect. 4 we present results for the fractions of elemental silicon and of water released into the gas phase by sputtering and by grain-grain collisions for each of a large number of shock models. Concluding remarks are in Sect. 5

2. The calculation of the grain-neutral and grain-grain relative speeds

We consider an oblique shock propagating at a velocity $-V_S\,\hat{z}$ relative to an upstream medium and measure all quantities in the frame comoving with the shock. Though many oblique C-type shocks may be time-dependent (Wardle 1991; Pilipp & Hartquist 1994, hereafter PH) we will assume that the flow in the shock frame is steady as a number of simplifying assumptions are necessary in order to make the current study tractable at this stage of our understanding of the evolution of oblique C-type shocks; in any case, even if the shocks possess time-dependent structures it is doubtful that the time averaged properties of their dissipation regions would contrast greatly with those given by the approach that we adopt.

The treatment we use is similar to that in the analytic sections of the paper by PH but contains modifications for the inclusion of a second grain fluid. ρ_j, n_j, v_j, and T_j denote the mass density, number density, velocity, and temperature of the jth fluid in the dissipation region; the fluids will be taken to be neutrals, ions, electrons, large grains, and small grains signified by the subscripts n, i, e, g, and s respectively. m_j is the mean mass of a particle in the jth fluid. $\boldsymbol{E}$ and $\boldsymbol{B}$ are the electric and magnetic fields. Subscripts x, y, and z mark the xth, yth, and zth components of a vector. The subscript o signifies the upstream value of a quantity. Grains are assumed to be spherical with radii of a_g and a_s; the mass density of the material composing the grains is taken to be 3 g cm^{-3} and the grains are assumed to be nonporous. $Z_g\,e$ and $Z_s\,e$ are the charges carried by each of the big and small grains respectively; e is the elementary charge, and q_j is the charge carried by each particle in the jth fluid. (Note that our q_j is a factor of e times the q_j of Pilipp et al. 1990 and PH.) The gyrofrequency $\Omega_j \equiv q_j\,B/m_j\,c$, where c is the speed of light. ν_{jn} is the collision frequency of particles in the jth fluid with neutrals defined so that $\boldsymbol{F}_j \equiv \rho_j\,\nu_{jn}\,(\boldsymbol{v}_n - \boldsymbol{v}_j)$ is the momentum transfer rate per unit volume to the jth fluid due to collisions with neutrals.

Upstream values of B_{xo}, B_{yo}=0, B_{zo}, and ρ_{no} and values of ρ_g/ρ_n, ρ_s/ρ_n, and B_x and B_y are assumed. The ionization balance was calculated from

$$n_i - n_e + n_s\,Z_s + n_g\,Z_g = 0 \quad (1)$$

$$\zeta\,n_n - n_g\,\Gamma_{eg} - n_s\,\Gamma_{es} = 0 \quad (2)$$

$$\Gamma_{ig} - \Gamma_{eg} = 0 \quad (3)$$

$$\Gamma_{is} - \Gamma_{es} = 0 \quad (4)$$

which yield n_i, n_e, Z_g, and Z_s for an input cosmic ray ionization rate, ζ, of 10^{-17} s^{-1}. Γ_{eg} and Γ_{es} are the electron currents onto big and small grains while Γ_{ig} and Γ_{is} are the ion currents onto big and small grains; these currents were evaluated following Havnes et al. (1987) with all sticking coefficients taken to be unity. A more extensive ionization structure calculation similar to that performed by Pilipp et al. (1990) was made to establish the validity of Eq. 2 in the parameter regimes we considered.

Equations (3) and (16) of PH were used to calculate velocities. ν_{en} was assumed to be zero in the electron equation of motion, but the other ν_{jn}'s were computed as in the work of Pilipp et al. (1990) and PH following Draine (1986); the expressions for ν_{gn} and ν_{sn} are appropriate for either totally elastic grain-neutral scattering or for collisions giving rise to specular reflection of the neutrals. From the assumption that the shock is steady, the $\hat{z}$ component of the current is constrained to be zero (cf. Eq. (11) of PH).

The electron and ion temperatures were calculated from Eq. (11) of Pilipp et al. (1990). In the temperature calculations we, as did Pilipp et al. (1990) and PH, evaluated ion-neutral and electron-neutral energy transfer rates following Draine(1986).

The $\hat{x}$ and $\hat{y}$ components of $\boldsymbol{E}$ are given by Eqns. (4d) and (4e) of PH. As is consistent with the assumption that ν_{en} can be set to zero in the electron equation of motion, E_z is calculated from Eq. (8b) of PH. $B_z = B_{zo}$ (cf. Eq. (4a) of PH).

The expression of the grain-neutral relative speed $\boldsymbol{v}_{jn} \equiv \boldsymbol{v}_j - \boldsymbol{v}_n$ (j=g, s) is then analogous to PH eqn. (9c). The grain-grain relative velocity is simply given by $\boldsymbol{v}_{gs} \equiv \boldsymbol{v}_{gn} - \boldsymbol{v}_{sn}$.

3. The sputtering and grain-grain collision induced silicon and water injection rates

The fraction of a small grain's mass and the fraction of a large grain's mass injected into the gas phase following the collision of a small grain with a big grain were calculated through the application of the procedure described in Sect. 3.3 of Tielens et al. (1994). Small grains and big grains were assumed to be composed of identical materials and a threshold grain-grain collision velocity for the injection of elemental silicon and water into the gas phase of 19 km s^{-1} and of 6.5 km s^{-1} were specified. We assumed that elemental silicon contains 20 percent of the evaporated mass of refractory material.

The rate per unit volume of collisions of small grains with big grains is

$$R_{gs} = n_s n_g \pi (a_g + a_s)^2 |\boldsymbol{v}_g - \boldsymbol{v}_s|. \quad (5)$$

We estimate (cf. Draine 1980) the length of the dissipation region, Δ, from

$$\frac{B_x^2 + B_y^2}{8\pi\Delta} = F_{iz} + F_{gz} + F_{sz} \quad (6)$$

which gives a reasonable agreement for Δ's obtained by Draine et al. (1983). If grains were not destroyed in collisions, the expected number of times that a small grain would be hit by a big grain while passing through the shock is given roughly by

$$N_s \approx 2R_{gs}\Delta/n_s V_S. \quad (7)$$

An analogous expression for the average number of times that a big grain would be hit by a small grain is

$$N_{\rm g} \approx 2R_{\rm gs}\Delta/n_{\rm g}V_{\rm S}. \quad (8)$$

In cases in which a small grain is totally destroyed in its first collision with a big grain, Poisson statistics have been applied. The above estimates of $N_{\rm s}$ and $N_{\rm g}$ were used in the calculation of the total mass of elemental silicon and the mass of water released per unit volume into the gas phase by grain-grain collisions in the shock.

The amount of grain mass injected into the gas phase due to the collision of a grain with a rapidly moving neutral gas particle was calculated with Eq. (27) of Draine & Salpeter (1979). Parameters given for silicates and water ice in Sect. 4.2.2 of Tielens et al. (1994) were used. To obtain a sputtering rate per unit volume we performed the appropriate averaging over the neutral velocity distribution function, which in the frame of a grain appears to be a velocity-shifted Maxwellian distribution characterized by $T_{\rm n}/m_{{\rm n}k}$ and $|\boldsymbol{v}_{\rm n} - \boldsymbol{v}_{\rm g}|$ or $|\boldsymbol{v}_{\rm n} - \boldsymbol{v}_{\rm s}|$; k specifies either H_2 or He since sputtering by both species and a $n({\rm He})/n({\rm H_2})$ ratio of 0.2 were assumed.

As in the evaluation of the mass of silicon or ice liberated by grain-grain collisions, $2\Delta/V_{\rm S}$ was taken as an estimate of the total time of passage through the dissipation zone in the calculation of the amount of silicon or ice sputtered. As mentioned above, appropriate averages over the neutral velocity distribution had to be calculated to get the silicon and ice sputtering rates per unit time per unit volume in the shock.

While in the study of elemental silicon return to the gas phase we assumed that the grains are composed entirely of silicates, in the study of H_2O return to the gas phase we supposed the ice to exist only in the mantles surrounding silicate cores. The fractional abundance (relative to H nuclei) of solid H_2O has been assumed to be 7.25×10^{-5}, as deduced from observations towards the Taurus complex (e.g. Whittet & Duley 1991). In our models, the numbers of water molecules on big and small grains ($N_{\rm H_2O}$(g) and $N_{\rm H_2O}$(s), respectively) are proportional to the number of surface sites for adsorption, i.e. $N_{\rm H_2O}({\rm g})/N_{\rm H_2O}({\rm s}) = (a_{\rm g}/a_{\rm s})^2$. For a Mathis et al. (1977; hereafter MRN) grain size distribution, $a_{\rm g} = 4 \times 10^{-5}$ cm, $a_{\rm s} = 4 \times 10^{-6}$ cm, a gas to dust ratio of 100 by mass, and a surface density of adsorbing sites of $1.5 \times 10^{15}{\rm cm}^{-2}$ (see Tielens & Allamandola 1987), the above assumptions imply an ice mantle thickness of $\sim 9 \times 10^{-7}$cm. In the calculation of water vaporization following grain-grain collisions and sputtering of water molecules, we therefore neglected the grain radius increase due to the presence of ice mantles. The equations used are as in the "bare" silicate case with silicate parameters replaced by ice parameters (cf. Tables 1 and 3 in Tielens et al. 1994). The density of the material composing dust grains was kept fixed at 3 g cm^{-3} (silicate density) because most of a grain's volume is filled by the silicate core.

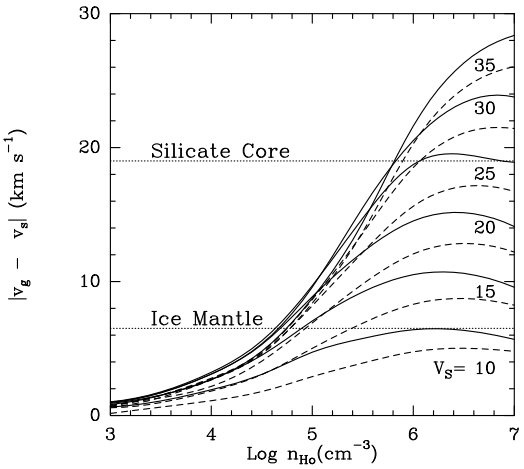

Fig. 1. Grain-grain relative speed. The speed of the shock labels each pair of curves. The solid curves are for $V_{\rm Ao}$ = 1.6 km s^{-1} and the dashed curves are for $V_{\rm Ao}$ = 3.1 km s^{-1}. The horizontal dotted lines show the thresholds for water and silicate vaporization.

4. Results

In most models $a_{\rm s} = 4 \times 10^{-6}$ cm, $a_{\rm g} = 4 \times 10^{-5}$ cm, $n_{\rm s} = 10^{2.5}\, n_{\rm g}$ (to simulate a MRN size distribution), and $(\rho_{\rm s}+\rho_{\rm g})/\rho_{\rm n} = 10^{-2}$. Also $B_{\rm x} = B_{\rm y}$ in all models and we specify $f_\perp \equiv (B_{\rm x}^2 + B_{\rm y}^2)^{1/2}/B_{\rm z}$ and assume for all models that $B_{\rm xo} = B_{\rm zo}$ with $B_{\rm yo} = 0$. In addition we specify $\rho_{\rm no}$, the upstream Alfvèn speed $V_{\rm Ao} \equiv [(B_{\rm xo}^2 + B_{\rm zo}^2)/4\pi\rho_{\rm no}]^{1/2}$ as well as the shock speed $V_{\rm S}$. A choice of $V_{\rm Ao}$ of 1.6 km s^{-1} is appropriate for a dark cloud while a value of $V_{\rm Ao}$ of 3.1 km s^{-1} is probably relevant for a region of high mass star formation, assuming that in molecular clouds the nonthermal kinetic energy density equals the magnetic energy density (e.g. Myers & Goodman 1988).

Fig. 1 presents the speed of big grains relative to small grains as a function of $n_{\rm Ho}$ (where $n_{\rm Ho}$ is the upstream hydrogen nuclei number density) and shock speed for two values of $V_{\rm Ao}$. The standard assumptions described in the first paragraph of this section were made and $f_\perp = 2.5\,(V_{\rm S}/25)/(V_{\rm Aox}/2.2)$ (which is characteristic of a large fraction of each dissipation region for which Draine et al. (1983) gave results). One sees that the higher value of $V_{\rm Ao}$ leads to lower relative speeds between big grains and small grains, that for $n_{\rm Ho} \gtrsim 5 \times 10^4$ cm^{-3} and $V_{\rm S} \gtrsim 10$ km s^{-1} the relative big grain - small grain speed exceeds the threshold speed for vaporization of water, and that for $n_{\rm Ho} \gtrsim 10^6$ cm^{-3} and $V_{\rm S} \gtrsim 25$ km s^{-1} the relative big grain - small grain speed exceeds the threshold speed for vaporization of silicates.

Values of $n_{\rm H}$ (the number density of hydrogen nuclei in the dissipation region), $n_{\rm e}$, $n_{\rm i}$, $Z_{\rm g}$, $Z_{\rm s}$, $\nu_{\rm gn}$, $\nu_{\rm sn}$, $T_{\rm e}$, and $T_{\rm i}$ for shock models with $n_{\rm Ho} = 10^6$ cm^{-3} and different shock speeds are listed in Table 1.

Fig. 2 displays the rates at which silicon atoms are sputtered from big grains and from small grains as functions of $V_{\rm S}$, $n_{\rm Ho}$, and $V_{\rm Ao}$. The same assumptions as those made for the production of Fig. 1 were used. The decreases in sputtering rates at large

Table 1. Results of shock models with $n_{\rm Ho} = 10^6\,{\rm cm}^{-3}$, $V_{\rm Ao} = 3.1\,{\rm km\ s}^{-1}$ (with $B_{\rm xo} = B_{\rm z}$ and $B_{\rm x} = B_{\rm y}$; $f_\perp = 2.5(V_{\rm S}/2.5)/(V_{\rm Aox}/2.2)$), $a_{\rm g} = 4 \times 10^{-5}$ cm, $a_{\rm s} = 4 \times 10^{-6}$ cm (with $n_{\rm s} = 10^{2.5} n_{\rm g}$ and $(\rho_{\rm g} + \rho_{\rm s})/\rho_{\rm n} = 0.01$), and different shock velocities.

$V_{\rm S}$ (km s^{-1})	$n_{\rm H}$ (cm^{-3})	$n_{\rm e}$ (cm^{-3})	$n_{\rm i}$ (cm^{-3})	$\nu_{\rm gn}$ (s^{-1})	$\nu_{\rm sn}$ (s^{-1})	$Z_{\rm g}$	$Z_{\rm s}$	$T_{\rm e}$ (K)	$T_{\rm i}$ (K)
10	1.00×10^{6}	5.68×10^{-3}	5.75×10^{-3}	5.02×10^{-9}	7.59×10^{-8}	-134	-15	1.54×10^{3}	4.24×10^{3}
20	1.02×10^{6}	6.00×10^{-3}	6.15×10^{-3}	1.26×10^{-8}	1.92×10^{-7}	-226	-28	3.02×10^{3}	2.65×10^{4}
30	1.02×10^{6}	7.07×10^{-3}	7.20×10^{-3}	2.37×10^{-8}	3.23×10^{-7}	-380	-49	5.29×10^{3}	7.37×10^{4}
40	1.02×10^{6}	8.52×10^{-3}	8.66×10^{-3}	3.88×10^{-8}	4.56×10^{-7}	-733	-87	9.50×10^{3}	1.45×10^{5}

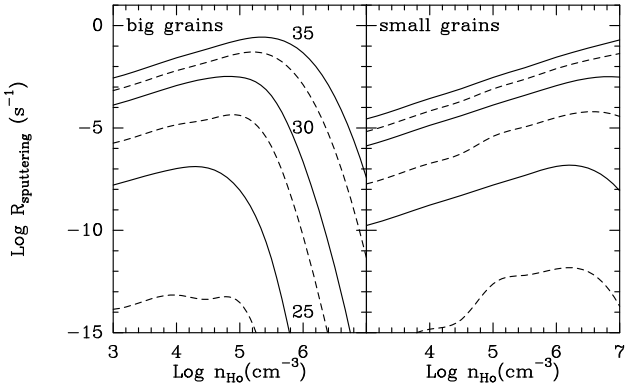

Fig. 2. Sputtering rates for silicates. The solid curves are for $V_{\rm Ao} = 1.6\,{\rm km\ s}^{-1}$ and the dashed curves are for $V_{\rm Ao} = 3.1\,{\rm km\ s}^{-1}$. The sputtering rate of big grains drastically decreases with increasing density for $n_{\rm Ho} \gtrsim 10^5\,{\rm cm}^{-3}$. On the other hand, the sputtering rate of small grains continues to increase up to larger densities before decreasing.

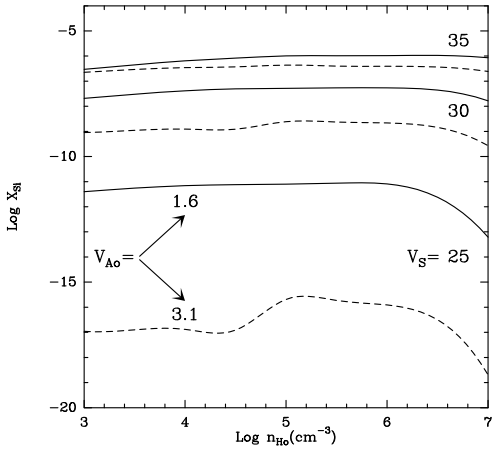

Fig. 3. Fractional abundance of elemental silicon injected into the gas phase as a result of sputtering. The solid curves are for $V_{\rm Ao} = 1.6\,{\rm km\ s}^{-1}$ and the dashed curves are for $V_{\rm Ao} = 3.1\,{\rm km\ s}^{-1}$.

values of $n_{\rm Ho}$ occur because at sufficiently high densities the friction between neutrals and grains is large enough to result in grains decoupling from the magnetic field and consequently to cause the grains to move at a velocity close to that of the neutrals. The gyrofrequency of a small grain is larger than that of a big grain by a factor of $(a_{\rm g}/a_{\rm s})^3$ while the ratio of stopping frequency of a big grain to that of a small grain scales as $(a_{\rm s}/a_{\rm g})$ for $v_{\rm g} = v_{\rm s}$; consequently, small grains remain better coupled than big grains to the magnetic field and the ion and electrons that move with it.

Fig. 3 contains results for the fractional abundance (relative to hydrogen nuclei) of elemental silicon injected into the gas phase by sputtering of grains. The same assumptions as those made for the production of Figs. 1 and 2 were used. Typical SiO fractional abundances observed toward molecular outflows range from about 10^{-9} to $\gtrsim 10^{-6}$ (e.g. Martín-Pintado et al. 1992). On the assumption that a substantial fraction of the sputtered silicon is efficiently converted to SiO (e.g. Neufeld & Dalgarno 1989; Herbst et al. 1989) or that SiO molecules are directly released into the gas phase by sputtering, good agreement with observations is then reached for $V_{\rm S} \gtrsim 30\,{\rm km\ s}^{-1}$. If $V_{\rm S} < 30\,{\rm km\ s}^{-1}$ grain sputtering is not capable of reproducing observed SiO gas phase abundances in the whole range of gas densities considered. As we will show later in this section, the fractional abundance of elemental silicon injected into the gas phase as a result of sputtering depends strongly on the number and size of the small grains. Note also in Fig. 3 the strong influence of the upstream magnetic field on sputtered silicon at shock speeds of about 25-30 km s^{-1}.

Fig. 4 shows the ratio $\beta_{\rm Si}$ of the amounts of elemental silicon injected into the gas phase as a consequence of grain-grain collisions and as a result of sputtering in the dissipation region of a shock propagating into a region with $n_{\rm Ho} = 3 \times 10^6\,{\rm cm}^{-3}$. Because $f_\perp$ actually varies throughout a dissipation region, we give results in this figure for two values of $f_\perp$. One of the values is $2.5\,(V_{\rm S}/25)/(V_{\rm Aox}/2.2)$ which we have used to produce results in all other figures in this paper because such a value is characteristic of most of a dissipation region according to fully spatially dependent steady shock models. The other value of $f_\perp$ is $5.0\,(V_{\rm S}/25)/(V_{\rm Aox}/2.2)$ which is very close to being large enough for the magnetic pressure to equal the total ram pressure of the shock and is, thus, nearly the highest value that obtains anywhere in the precursor. We consider the results for $f_\perp = 2.5\,(V_{\rm S}/25)/(V_{\rm Aox}/2.2)$ to give a reasonable approximation to the values that one would obtain in a corresponding fully spatially dependent model of a dissipation region, while the results for $f_\perp = 5.0\,(V_{\rm S}/25)/(V_{\rm Aox}/2.2)$ give a strict lower bound

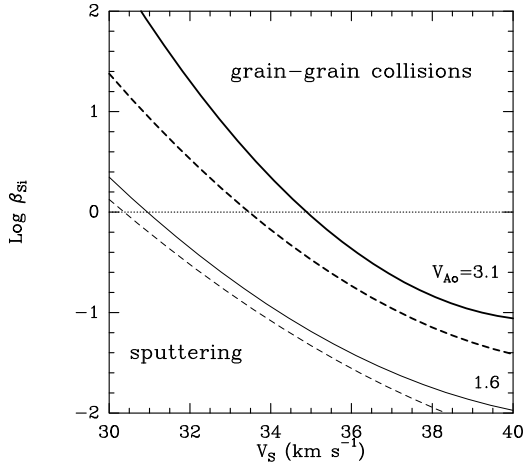

Fig. 4. Ratio of gas phase elemental silicon produced by grain-grain collisions to that produced by sputtering in the dissipation region of a shock propagating into a region with $n_{\rm Ho} = 3 \times 10^6$ cm^{-3}. Thick curves are for $V_{\rm Ao} = 3.1$ km s^{-1} and thin curves are for $V_{\rm Ao} = 1.6$ km s^{-1}. Solid curves are for $f_\perp = 2.5\,(V_{\rm S}/25)/(V_{\rm Aox}/2.2)$, and dashed curves are for $f_\perp = 5.0\,(V_{\rm S}/25)/(V_{\rm Aox}/2.2)$.

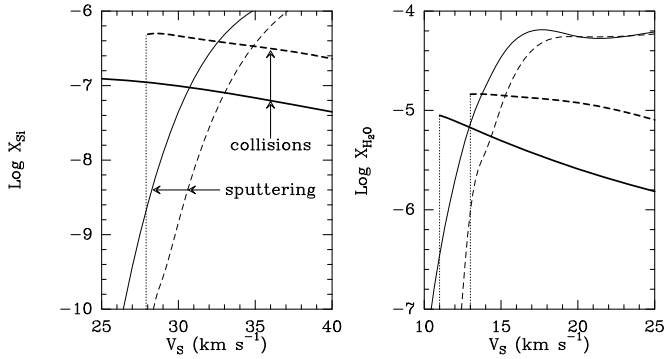

Fig. 5. Gas phase fractional abundances of elemental silicon and of H_2O produced by grain-grain collisions (thick curves) and by sputtering (thin curves) behind shocks ahead of which $n_{\rm Ho} = 3 \times 10^6$ cm^{-3}. All other parameters were assumed to have the same values as those used in the production of Figs. 1 through 3; in particular, solid curves refer to models with $V_{\rm Ao} = 1.6$ km s^{-1}, and dashed curves are for $V_{\rm Ao} = 3.1$ km s^{-1}. Dotted lines mark shock speed values below which grain relative speeds are below vaporization threshold.

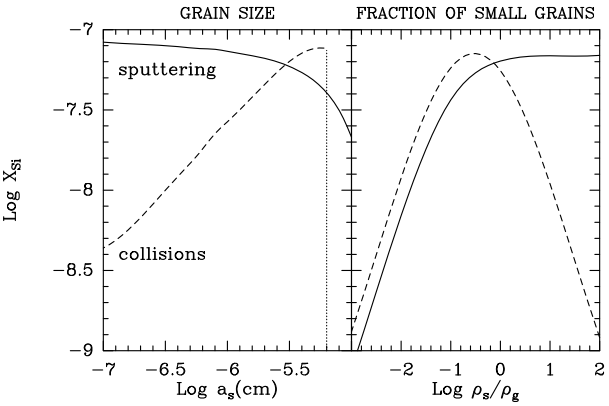

Fig. 6. The dependance of the fractional abundances of gas phase elemental silicon produced by grain-grain collisions (dashed curves) and by sputtering (solid curves) on $a_{\rm s}$ (left figure) and $\rho_{\rm s}/\rho_{\rm g}$ (right figure). $V_{\rm S} = 30$ km s^{-1}, $n_{\rm Ho} = 1 \times 10^6$ cm^{-3}, and $V_{\rm Ao} = 1.6$ km s^{-1}.

to the ratio of elemental silicon production by grain-grain collisions to that by sputtering.

Grain-grain collisions are more efficient than sputtering at low shock velocities ($V_{\rm S} \lesssim 35$ km s^{-1} if $V_{\rm Ao} = 3.1$ km s^{-1}, and $V_{\rm S} \lesssim 30$ km s^{-1} if $V_{\rm Ao} = 1.6$ km s^{-1}; see Fig. 4). At gas densities lower than about 10^6 cm^{-3} and shock velocities $V_{\rm S} < 25$ km s^{-1}, grain-grain collisions are not energetic enough to vaporize silicate grains (cf. Fig. 1). This is also shown in Fig. 5 which gives results for the gas phase fractional abundances (relative to hydrogen nuclei) of elemental silicon, $X_{\rm Si}$, and water, $X_{\rm H_2O}$, resulting from grain-grain collisions only and from sputtering only behind shocks with $n_{\rm Ho} = 3 \times 10^6$ cm^{-3}. In the case of water, grain-grain collisions dominate over sputtering in a narrow range of low shock speeds ($V_{\rm S} \sim 11 - 15$ km s^{-1}). Below a shock speed of about 11 km s^{-1} a small fraction (< 0.1 %) of the frozen H_2O molecules are released into the gas phase only by sputtering.

Fig. 6 displays the dependences on the small grain size and number of the fractional abundances of silicon produced by grain-grain collisions and sputtering in shocks with $V_{\rm S} = 30$ km s^{-1} and propagating into a medium with $n_{\rm Ho} = 1 \times 10^6$ cm^{-3} and $V_{\rm Ao} = 1.6$ km s^{-1}. For the plot on the left hand side of the figure the ratio of the mass contained in small grains to the mass contained in large grains is $10^{-0.5}$. For the plot on the right hand side of the figure $a_{\rm s} = 4 \times 10^{-6}$ cm and $(\rho_{\rm s} + \rho_{\rm g})/\rho_{\rm n} = 0.01$. Otherwise, the parameters assumed for the generation of the figures were taken to be those used for the production of Fig. 1. $X_{\rm Si}$ produced by grain-grain collisions is small when $\rho_{\rm s}/\rho_{\rm g}$ is very different from unity. This is due to the fact that high speed collisions occur mostly between grains of different sizes. The amount of material which can be returned to the gas by grain-grain collisions is therefore limited by the grain component containing the smaller amount of mass. Thus the maximum effect of grain-grain collisions is reached when both components contain about equal amount of mass. This is clearly seen in Fig. 6. Since sputtering works efficient on small grains because of their large surface area, grain destruction is dominated by sputtering once the small grains dominate the grain population.

5. Conclusions

Our results show that there exists a shock parameter regime in which small grain - big grain collisions release more elemental silicon into the gas phase than sputtering of grains does. For an assumed large grain radius of $a_{\rm g} = 4 \times 10^{-5}$ cm and values of other parameters taken to be appropriate for star forming regions, $n_{\rm Ho}$ must be at least about 5×10^5 cm^{-3} and 25 km s^{-1} $\lesssim V_{\rm S} \lesssim 35$ km s^{-1} for grain - grain collisions to

dominate over sputtering for the production of gas phase elemental silicon.

Because of the high preshock densities involved, grain-grain collisions will probably operate in regions of high mass star formation. It is interesting to note that fractional abundances of gas phase silicon of at least 10^{-6} have been deduced from SiO observations towards outflows around low mass young stellar objects (e.g. Martín-Pintado et al. 1992; Avery & Chiao 1996). Grain-grain collisions by themselves are then unlikely to be responsible for the injection of elemental silicon into the gas phase in low mass star forming regions (cf. Figs. 5 and 6). On the other hand, grain-grain collisions are capable of producing fractional abundances of gas phase silicon at least comparable to those measured to be contained in gas phase SiO in regions of high mass star formation where $X_{\rm SiO} \simeq 10^{-9} - 10^{-8}$ (e.g. Martín-Pintado et al. 1992; Acord et al. 1996).

Grain-grain collisions dominate over sputtering in the return of water to the gas phase only in a narrow range of shock speeds below about 15 km s^{-1} (Fig. 5). Ice mantles of dust grains are completely released into the gas phase by sputtering if $V_{\rm S} \gtrsim 15\,{\rm km\ s^{-1}}$ and in the whole density range considered ($10^3 \leq n_{\rm Ho} \leq 10^7\ {\rm cm^{-3}}$). Given that water molecules are bound to grain surfaces more strongly than other typical compounds of grain mantles (e.g. methanol, methane, ammonia; see Tielens & Allamandola 1987), we also expect enhanced gas phase fractional abundances of molecules such as CH_3OH and NH_3 after the passage of the shock even at shock speeds as low as $\sim 10\,{\rm km\ s^{-1}}$.

In the present work we have concentrated on the development of the first model of the dissipation regions in C-type shocks including more than a single grain fluid in order to calculate grain-grain collision rates and speeds in such shocks for the first time. In the future our investigations could be expected to include a consideration of the chemical forms in which grain-grain collisions and grain sputtering introduce silicon and frozen molecules into the gas phase and the subsequent gas phase chemistry; gas phase silicon chemistry has been investigated by Schilke et al. (1996) for cases in which sputtering (induced by more massive gas phase neutrals as well as H_2 and He) is the sole important mechanism for returning elemental silicon to the gas phase.

Acknowledgements. Constructive suggestions made by Dr. Carsten Dominik led to the improvement of the paper's presentation. This work has been supported in part by a grant from the Research Council of Norway and by the Commission of the European Union (Brussels) through the "Colloidal Plasmas" network of the Human Capital and Mobility Program under contract No. ER-BCHRXCT94062

References

Acord J. M., Walmsley C. M., Churchwell E. B. 1996, A&A, in press
Avery L. W. Chiao, M. 1996, ApJ, 463, 642
Bally J., Lada E. A., Lane A. P. 1993, ApJ, 418, 322
Blake G. A., Sandell G., van Dishoeck E. F., Groesbeck T. D., Mundy L. G., Aspin C. 1995, ApJ, 441, 689
Downes D., Genzel R., Hjalmarson Å., Nyman L. Å., Rönnäng B. 1982, ApJ, 252, L29
Draine B. T., Salpeter E. E. 1979, ApJ, 231, 77
Draine B. T. 1980, ApJ, 241, 1021
Draine B. T., Roberge W. G., Dalgarno A. 1983, ApJ, 264, 485
Draine B. T. 1986, MNRAS, 220, 133
Draine B. T. 1995, Ap&SS, 233, 111
Flower D. R., Pineau des Forêts G. 1995, MNRAS, 275, 1049
Havnes O., Hartquist T. W., Pilipp W. 1987, in: Physical Processes in Interstellar Clouds, eds. G. E. Morfill, M. Scholer, D. Reidel Publishing Company, p. 389
Herbst E., Millar T. J., Wlodek S., Bohme D. K. 1989, A&A, 222, 205
Jones A. P., Tielens A. G. G. M., Hollenbach D. J., McKee C. F. 1994, ApJ, 433, 797
Jones A. P., Tielens A. G. G. M. Hollenbach D. J. 1996, ApJ, in press
Martín-Pintado J., Bachiller R., Fuente A. 1992, A&A, 254, 315
Mathis J. S., Rumpl W., Nordsieck K. H. 1977, ApJ, 217, 425
McMullin J. P., Mundy L. G., Blake G. A. 1994, ApJ, 437, 305
Mikami H., Umemoto T., Yamamoto S., Saito, S. 1992, ApJ, 392, L87
Myers P. C., Goodman A. A. 1988, ApJ, 329, 392
Neufeld D. A., Dalgarno A. 1989, ApJ, 340, 869
Pilipp W., Hartquist T. W. 1994, MNRAS, 267, 801
Pilipp W., Hartquist T. W., Havnes, O. 1990, MNRAS, 243, 685
Schilke P., Walmsley C. M., Pineau des Forêts, G., Flower, D. R. 1996, A&A, in press
Seab C. G., Shull J. M. 1983, ApJ, 275, 652
Tielens A. G. G. M., Allamandola L. J. 1987, in: Interstellar Processes, eds. D. J. Hollenbach, H. A. Thronson, Jr., Dordrecht: Kluwer, p. 397
Tielens A. G. G. M., McKee C. F., Seab, C. G., Hollenbach, D. J. 1994, ApJ, 431, 321
Wardle M. 1991, MNRAS, 251, 119
Whittet D. C. B., Duley W. W. 1991, A&A Rev., 2, 167
Wright M. C. H., Plambeck R. L., Vogel, S. N., Ho, P. T. P., Welch, W. J. 1983, ApJ, 267, L41
Zhang Q., Ho P. T. P., Wright M. C. H., Wilner D. J. 1995, ApJ, 451, L71
Ziurys L. M., Friberg P., Irvine W. M. 1989, ApJ, 343, 201

This article was processed by the author using Springer-Verlag LaTeX A&A style file *L-AA* version 3.